International Journal of Heat and Mass Transfer 52 (2009) 5512–5524

Contents lists available at ScienceDirect

International Journal of Heat and Mass Transfer

journal homepage: www.elsevier.com/locate/ijhmt

Unsteady conjugate water/air mixed convection in a square cavity

Nelson O. Moraga [a,*], José A. Riquelme [a], Leopoldo A. Jauriat [b]

[a] Mechanical Engineering Department, Universidad de Santiago de Chile, Alameda 3363, Santiago, Chile
[b] Mechanical Engineering Department, Universidad de Antofagasta, Av. Angamos 601, Antofagasta, Chile

ARTICLE INFO

Article history:
Received 16 October 2008
Received in revised form 17 June 2009
Accepted 17 June 2009
Available online 18 August 2009

Keywords:
Transient conjugate convection
Finite volume simulation
Heat transfer
Fluid dynamics

ABSTRACT

Transient natural convection inside an inner thin walled container caused by external mixed convection in a square cavity has been analyzed numerically. Air and water were chosen alternatively as internal and external working fluids. Fluid mechanics and conjugate heat transfer, described in terms of continuity, linear momentum and energy equations, were predicted by using the finite volume method. Streamlines, isotherms, velocity profiles and local Nusselt number time evolution are presented for external flows, of either air or water, with Ri = 1, in two cases: Re = 200 and 500.

1. Introduction

Natural, forced and mixed convective flows in rectangular enclosures are often found in natural and industrial processes. The knowledge of fluid dynamics and transient mixed convective heat transfer is essential to improve many technological applications such as microelectronic cooling devices, heat exchangers, solar energy collectors, building heating and ventilation systems, air and water contamination removal from cavities [1] and food heating and cooling devices [2].

Natural convection in cooling equipments has been investigated previously [3–5]. Sathe and Joshi [6] reported a parametric study for natural convection inside a rectangular cavity with a liquid being cooled by a solid protruding inside the cavity. Dielectric liquids were found to enhance the cooling rate by air when the protuberance material thermal conductivity was higher than the liquid. Ganzarolli and Milanez [7] studied natural convection in a rectangular cavity being heated from the bottom and symmetrically cooled from the lateral walls. The numerical results show that the Nusselt number was a function of the Rayleigh number with a weak contribution of the Prandtl number.

Ledezma and Bejan [8] studied the best location for vertical fins in order to enhance natural convection. An improvement in cooling was obtained with an internal architecture for the fins with a given volume that allowed minimizing the global thermal resistance. Armield and Janssen [9] by introducing an artificial perturbation in a cavity investigated the stationary convection boundary layer stability. Hamady et al. [10] investigated natural convection local heat transfer in an inclined cavity. They found the influence of the Rayleigh number and the inclination angle in the heat flux. Shuja et al. [11] investigated the entropy production in a cavity with a steel square body generating uniform heat, being cooled by either an air or a water flow. They found that a minimum value for the irreversibility ratio is obtained when the solid is located at the center of the cavity. Dagtekin and Oztop [12] studied the effect of fin sizes on the natural convection in a cavity. They showed that the mean Nusselt number depends on the fin length, with the fin location having stronger influence on the fluid mechanics than on the heat transfer. Similar numerical investigations for natural convection with three or a series of heat generating components in various position arrangements were carried out by Chuang et al. and Bhoite et al. [13,14]. Natural convection in partly divided cavities was studied by Yucel and Ozdem [15]. They showed that the flow velocity decreased as the partition height increased, with a reduction in the Nusselt number. Natural convection in a square cavity with a thin fin located in the hot wall was investigated by using different numerical techniques by Shi and Khodadadi [16], and by Tasnim and Collins [17]. They found that a fin normal to the hot wall modifies the fluid circulation, changing the vortex center location and they obtained an expression for the Nusselt number. Varol et al. [18] studied natural heat transfer and fluid mechanics due to the insertion of a heated protruding solid element in a triangular enclosure. They demonstrated that the location, height and width of the heater have important effects on heat transfer and fluid flow. A conjugate numerical study for natural convection heat conduction in an air-filled cavity with a centered solid was conducted by Deng and Tang [19], for $10^3 \leqslant Ra \leqslant 10^6$. They showed that results by dimensionless streamlines and heat lines directly exhibit the fluid flow and heat transfer nature at a macroscopic level for conjugate heat and mass transfer.

* Corresponding author. Tel.: +562 718 3118; fax: +562 682 3020.
E-mail address: nelson.moraga@usach.cl (N.O. Moraga).

0017-9310/$ - see front matter © 2009 Elsevier Ltd. All rights reserved.
doi:10.1016/j.ijheatmasstransfer.2009.06.030

Nomenclature

d	height of the opening (m)
g	gravitational acceleration (m/s^2)
Gr	Grashof number (=$g\beta\Delta TL^3/\nu^2$)
k	thermal conductivity (W/m K)
L	height of the cavity (m)
Nu	Nusselt number
P	dimensionless pressure
p	pressure
Pr	Prandtl number (=ν/α)
Re	Reynolds number (=LU_{in}/ν)
Ri	Richardson number (=Gr/Re^2)
Ra	Rayleigh number (=$g\beta\Delta TL^3/\nu\alpha$)
U, V	dimensionless velocity components
u, v	velocity components (m/s)
X, Y	dimensionless coordinates
x, y	coordinates (m)
T	temperature (K)
t	time (s)

Greek symbols

α	thermal diffusivity (m^2/s)
β	thermal expansion coefficient (1/K)
θ	dimensionless temperature
μ	dynamic viscosity (Pa s)
ν	kinematic viscosity (m^2/s)
ϕ	current variable (velocity component and temperature)
τ	dimensionless time

Subscripts

C	cold
H	hot
a	air
w	water
s	solid
I, J	node position
in	inlet

Superscripts

$n-1, n$	iteration number
$*$	parameter

Mixed convective flows in cavities have been studied by using analytical, experimental and numerical methods [20]. Papanicolau and Jaluria [21–23] studied an insulated cavity with a heat source and lateral inlet and outlet. They found that higher cooling rates are obtained when the outlet is at the bottom of the vertical wall [21,22]. Results were obtained with a stream–velocity formulation and the k–ε turbulence model [23]. Lee et al. [24] described the fluid flow and heat transfer for laminar and turbulent flows in a room being cooled by air, for Re = 10^4 and Ri = 0.1. Raji and Hasnaoui [25–28] reported numerical results to describe mixed convection in air inside a rectangular cavity including radiation for $10^3 \leqslant Ra \leqslant 5 \times 10^6$ and $5 \leqslant Re \leqslant 5000$. Omri and Nasrallah [29] using triangular elements with a control volume finite element method described mixed convection in an air-cooled square cavity, for $0.1 \leqslant Ri \leqslant 18$, $10 \leqslant Re \leqslant 500$. Mixed three-dimensional convection inside a cubical cavity cooled by air was studied by Moraga and López [30]. They found than a 3D model must be used to describe the fluid mechanics when Ri = 10 and $10 \leqslant Re \leqslant 250$ and to calculate the global Nusselt number for Re = 500 when Ri < 1. Steady forced convection inside a square cavity with inlet and outlet parts of different sizes was investigated for a total of 108 cases by Saeidi and Khodadadi [31]. They described the effect of inlet and outlet size and location on the pressure of clockwise and counter-clockwise primary and secondary vortices. Results indicated that inlet and outlet ports should be placed parallel to each other in order to minimize pressure drop. Shuja et al. [32] studied mixed convection in a cavity with a centered solid body with heat generation for 15 different outlet ports. They found a non-uniform cooling process, with decreased heat transfer and increased irreversibility, for 13 outlet ports.

The objective of the present work is to examine the characteristics of the fluid flow and heat transfer for unsteady natural convection induced in a centered fluid filled container by mixed convection of a different fluid external flow. Air and water are considered as either the internal or the external fluids. The fluid inside the container initially is at a higher temperature and is being cooled by the external cold fluid. The non-dimensional continuity, linear momentum and energy equations for the conjugate mixed/natural convection are solved by using the finite volume method, for Ri = 1 and Re = 200 and 500.

2. Physical situation

The conjugate mixed convection/natural convection inside a square cavity considered in this paper is shown in Fig. 1. The height

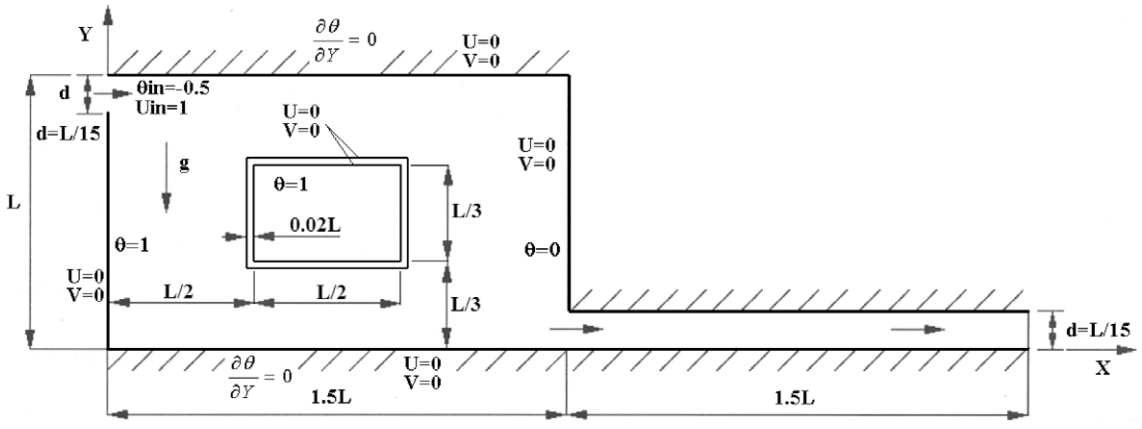

Fig. 1. Physical situation for conjugate water/air mixed convection in a square cavity.

and width are denoted by H and L, respectively. The problem is assumed to be two-dimensional due to the large depth of the enclosure. The fluid enters the cavity through the inlet port of width $d = L/15$, located on the upper section of the left vertical wall. The outlet port, located on the bottom section of the right vertical wall is extended a length equal to $1.5L$ to guarantee the use of outlet developed boundary conditions for the fluid flow and heat transfer. The inlet dimensionless temperature of the fluid is $\theta_{in} = -0.5$, with inlet dimensionless velocity components $U_{in} = 1$, $V_{in} = 0$. The left and right vertical walls are isothermal at dimensionless temperatures of $\theta_H = 1$ and $\theta_C = 0$, respectively, whereas the horizontal walls are adiabatic.

In the cavity center a square solid container with thin walls ($0.02L$ in wall thickness) is filled with fluid, that can be either air, when the external fluid is water, or water when the external fluid is air.

3. Mathematical model

The conjugate mixed convection with internal natural convection inside an inner square cavity is studied under the assumptions of laminar flow for constant properties incompressible Newtonian fluids. Only density is allowed to change linearly with temperature according to Boussinesq approximation.

The dimensionless dependent and independent variables are defined in the usual way:

$$U = \frac{u}{U_{in}}, \quad V = \frac{v}{U_{in}}, \quad P = \frac{p}{\rho U_{in}^2}, \quad \theta = \frac{T - T_C}{T_H - T_C} \tag{1}$$

$$X = \frac{x}{L}, \quad Y = \frac{y}{L}, \quad \tau = \frac{tU_{in}}{L} \tag{2}$$

The dimensionless coupled partial differential equations for the conservation of mass, linear momentum and energy are:

$$\frac{\partial U_i}{\partial X} + \frac{\partial V_i}{\partial Y} = 0 \tag{3}$$

$$\frac{\partial U_i}{\partial \tau} + \left[U_i \frac{\partial U_i}{\partial X} + V_i \frac{\partial U_i}{\partial Y}\right] = -\frac{\partial P_i}{\partial X} + \frac{1}{\mathrm{Re}}\left[\frac{\partial^2 U_i}{\partial X^2} + \frac{\partial^2 U_i}{\partial Y^2}\right] \tag{4}$$

$$\frac{\partial V_i}{\partial \tau} + \left[U_i \frac{\partial V_i}{\partial X} + V_i \frac{\partial V_i}{\partial Y}\right] = -\frac{\partial P_i}{\partial Y} + \frac{1}{\mathrm{Re}}\left[\frac{\partial^2 V_i}{\partial X^2} + \frac{\partial^2 V_i}{\partial Y^2}\right] + \mathrm{Ri}\theta \tag{5}$$

$$\frac{\partial \theta_i}{\partial \tau} + \left[U_i \frac{\partial \theta_i}{\partial X} + V_i \frac{\partial \theta_i}{\partial Y}\right] = \frac{1}{\mathrm{RePr}}\left[\frac{\partial^2 \theta_i}{\partial X^2} + \frac{\partial^2 \theta_i}{\partial Y^2}\right] \tag{6}$$

$$\frac{\partial \theta_s}{\partial \tau} = \alpha^*\left[\frac{\partial^2 \theta_s}{\partial X^2} + \frac{\partial^2 \theta_s}{\partial Y^2}\right] \tag{7}$$

$$\alpha^* = \frac{\alpha_s}{\alpha_a} \tag{8}$$

where the sub-index i is used to define the type of fluid: $i = a$ and w for air and water, respectively, and s for the solid walls of the container.

The non-dimensional Richardson, Prandtl, Grashof and Reynolds numbers are defined as follows:

$$\mathrm{Ri} = \frac{\mathrm{Gr}}{\mathrm{Re}^2}, \quad \mathrm{Pr} = \frac{v}{\alpha}, \quad \mathrm{Gr} = \frac{g\beta L^3 (T_H - T_C)}{v^2}, \quad \mathrm{Re} = \frac{LU_{in}}{v} \tag{9}$$

The boundary conditions for the fluid mechanicals are: a uniform horizontal velocity at the inlet port, no-slip at the solid walls for both external cavity and internal container and fully developed flow at the outlet port. Heat transfer boundary conditions include a dimensionless uniform inlet temperature for the cold fluid, $\theta_{in} = -0.5$, uniform hot and cold temperature on the vertical left and right walls, adiabatic horizontal walls and thermally fully developed flow at the outlet

$$\mathrm{Inlet}(X = 0) \quad U_{in} = 1, \quad V_{in} = 0, \quad \theta_{in} = -0.5 \tag{10}$$

$$\mathrm{Outlet}(X = 3), \quad \frac{\partial \theta}{\partial X} = 0, \quad \frac{\partial U}{\partial X} = 0, \quad V = 0 \tag{11}$$

Cavity and internal container walls

$$U = V = 0 \quad \theta(X = 0, Y) = 1 \quad \theta(X = 1.5, Y) = 0 \tag{12}$$

Cavity horizontal walls

$$\left.\frac{\partial \theta}{\partial Y}\right|_{Y=0;1} = 0 \tag{13}$$

Fluid–container interfaces

$$\left.\frac{\partial \theta_s}{\partial X}\right|_{wall} = \left.\frac{\partial \theta_{a,w}}{\partial X}\right|_{wall}, \quad \left.\frac{\partial \theta_s}{\partial Y}\right|_{wall} = \left.\frac{\partial \theta_{a,w}}{\partial Y}\right|_{wall}, \quad \theta_s|_{wall} = \theta_{a,w}|_{wall} \tag{14}$$

The initial condition inside the cavity considers that temperature varies linearly with the axial horizontal coordinate.

$$\theta(X) = 1 - \frac{X}{1.5} \tag{15}$$

Dimensionless heat transfer on the cavity and internal fluid container walls was computed by local and average Nusselt number in terms of the dimensionless temperature gradients between the walls and the surrounding fluid,

$$\mathrm{Nu}_{local}(Y) = \left.\frac{\partial \theta}{\partial X}\right|_{wall}, \qquad \mathrm{Nu}_{local}(X) = \left.\frac{\partial \theta}{\partial Y}\right|_{wall} \tag{16}$$

$$\overline{\mathrm{Nu}}(Y) = \int \mathrm{Nu}_{local}(Y)dY, \qquad \overline{\mathrm{Nu}}(X) = \int \mathrm{Nu}_{local}(X)dX \tag{17}$$

4. Solution procedure

The governing coupled equations (Eqs. (3)–(8)) with the initial and boundary conditions (Eqs. (10)–(15)) were solved with the finite volume method, FVM, by using the SIMPLE algorithm [33]. A two-dimensional non-uniform spaced staggered grid with 120×120 nodes, with 52×30 nodes located in the inner container and four nodes in the container walls, was used to discretize the physical domain. A higher nodes density near the cavity and internal container walls was used as it is shown in Fig. 2. Several grids with different sizes were used to solve the problem. Fig. 3 shows results for the horizontal velocity component, temperature and for the local Nusselt number on the hot wall calculated with three grids: 100×90, 120×100 and 120×120 nodes. A grid independent solution was found with a mesh of 120×120 nodes, for $\mathrm{Ri} = 1$ and $200 \leqslant \mathrm{Re} \leqslant 500$. A fifth power law was used to calculate the convective terms while the diffusion terms were determined by using linear interpolation functions for the dependent variables between the nodes.

Under-relaxation was used during the iterative process in the calculation of the improved values of the dependent primitive variables. The under-relaxations factors used for the two velocity components, temperature and pressure were.

$$\alpha_U = 0.4, \quad \alpha_V = 0.4, \quad \alpha_\theta = 0.7, \quad \alpha_P = 0.2 \tag{18}$$

The convergence criteria applied to stop the velocity and temperature calculations at each time step was based in a maximum value for the difference in the calculated value at two successive iterations, defined as follows

$$|\phi_{I,J}^n - \phi_{I,J}^{n-1}| \leqslant 10^{-4} \tag{19}$$

5. Results and discussion

A preliminary study was conducted to validate the method of present solution. First, the mixed convection in an air-cooled cavity

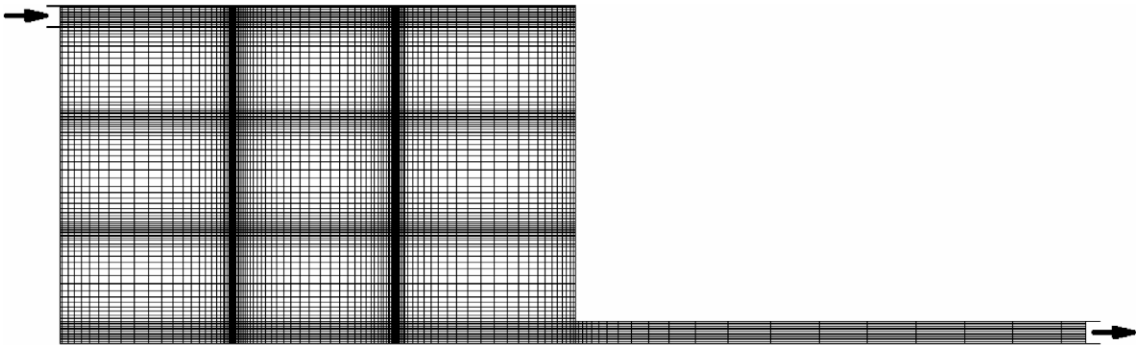

Fig. 2. Grid distribution of computational domain (120 × 120 nodes).

was predicted as a limiting case without a centered fluid container. Results for steady streamlines and isotherms lines were carefully examined with previous results for Re = 500, Ri = 1 obtained by Omri and Nasrallah [29] with the control volume finite element (CVFEM) and by Moraga and López [30] with the FVM and a grid with 110 × 80 nodes. Overall agreement for the absolute value of stream function and isotherm lines was excellent and some minor differences noticed near the outlet can be explained by the use of a different grid in present calculations (120 × 120 nodes).

The conjugate natural convection with heat conduction problem in an air-filled square cavity with a centered solid body inves-

Table 1
Average Nusselt number for natural convection in an air-filled cavity with a center solid body.

Ra	$\overline{Nu}$	
	Present	Deng and Tang [19]
10^3	1.299	1.418
10^4	1.721	1.794
10^5	4.302	4.372
10^6	8.578	8.57

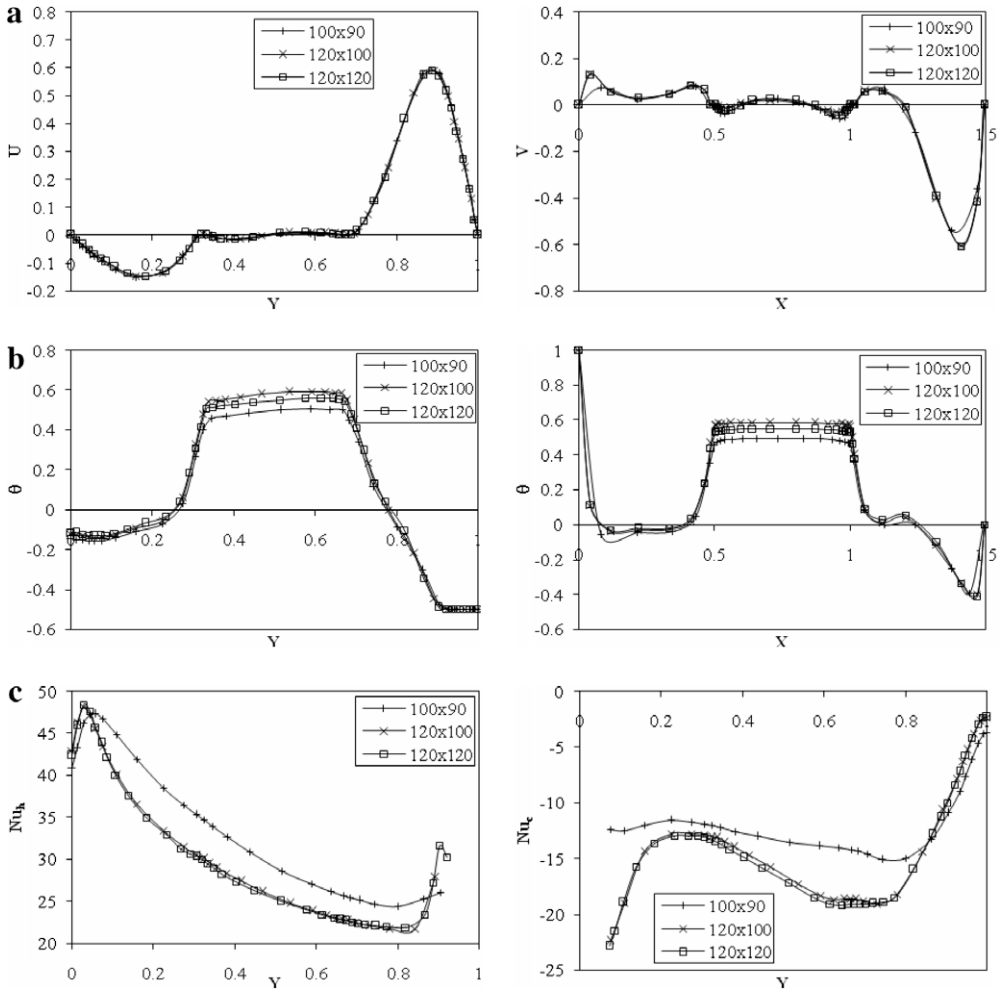

Fig. 3. Velocity (a) and temperature (b) profiles at mid vertical and horizontal cavity planes and (c) local Nusselt numbers on the vertical cavity walls, calculated with 100 × 90, 120 × 100 and 120 × 120 nodes.

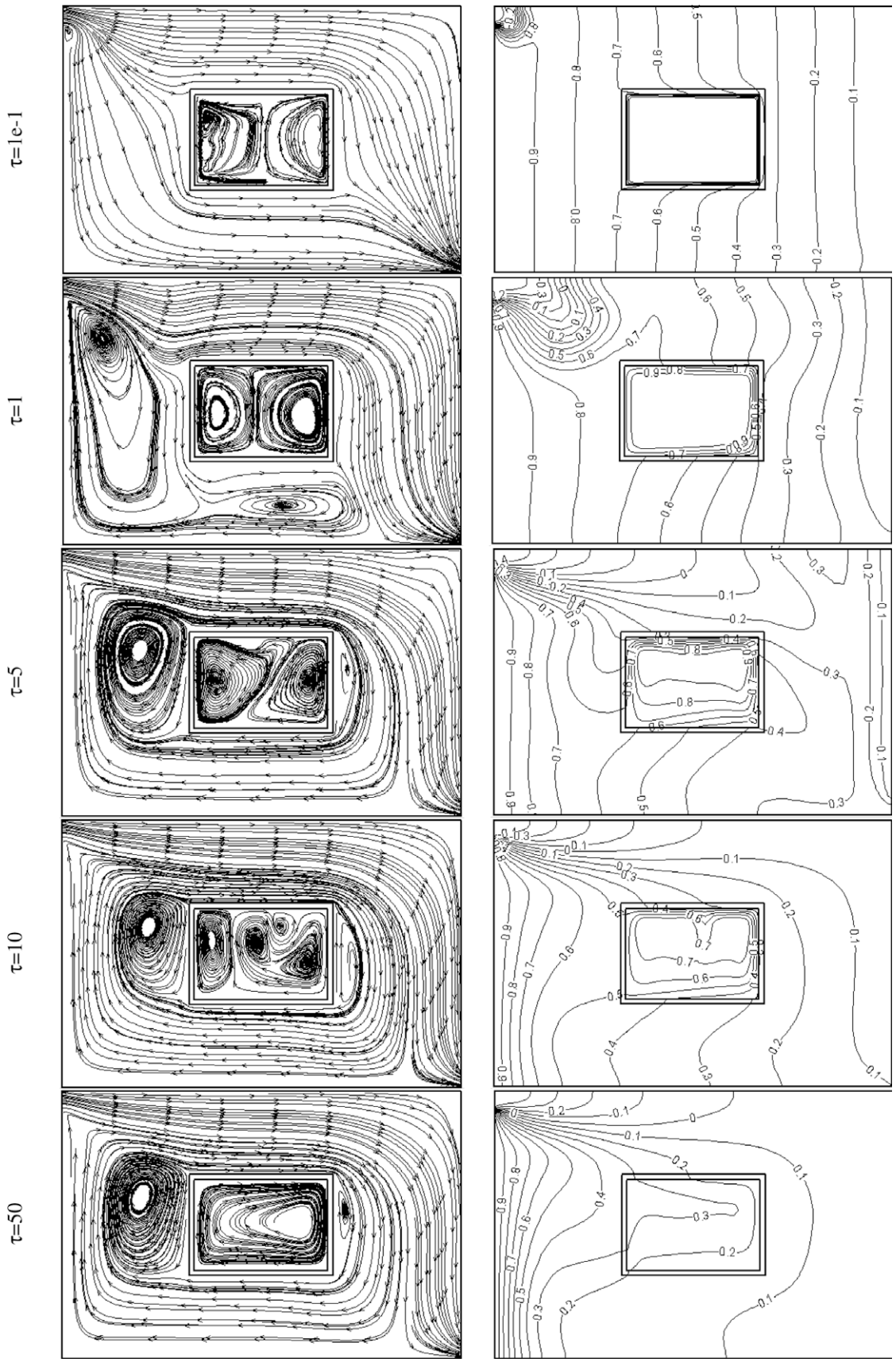

Fig. 4. Time variation of streamlines (left side) and distribution of temperature (right side), when the water in the container was cooled by air and Re = 200.

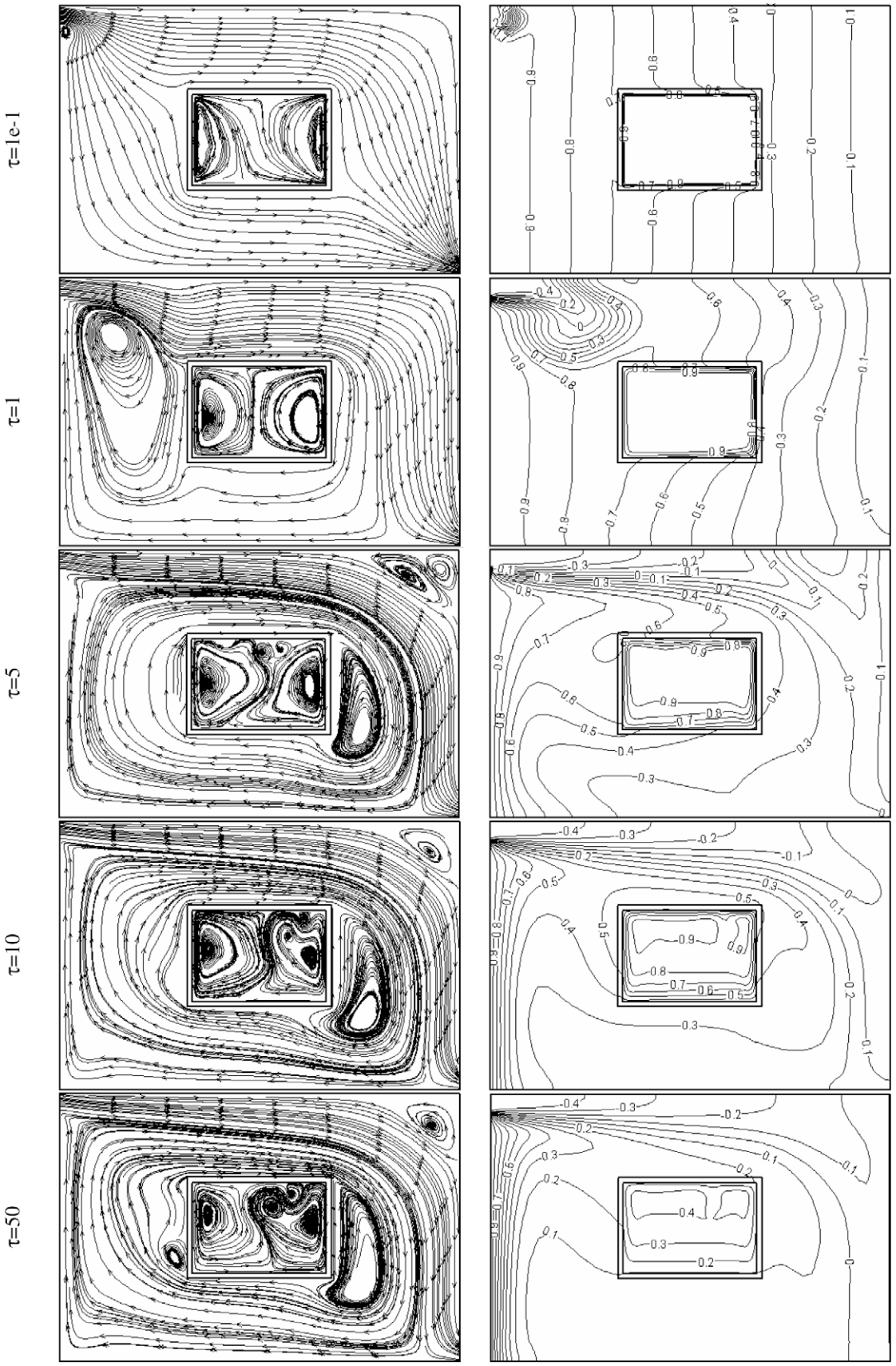

Fig. 5. Time variation of streamlines (left side) and distribution of temperature (right side), when the water in the container was cooled by air and Re = 500.

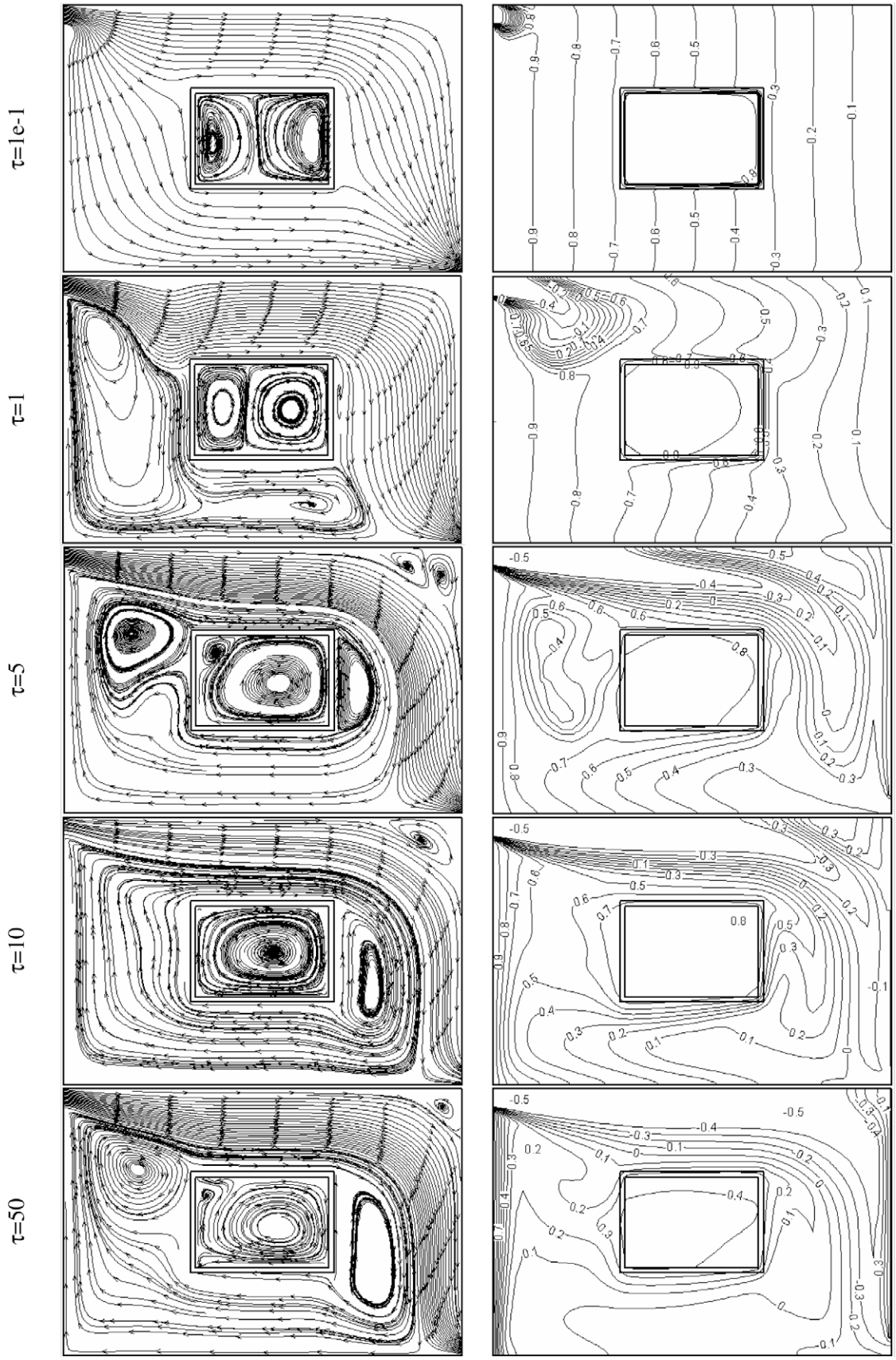

Fig. 6. Time variation of streamlines (left side) and distribution of temperature (right side), when the air in the container is cooled by water and Re = 200.

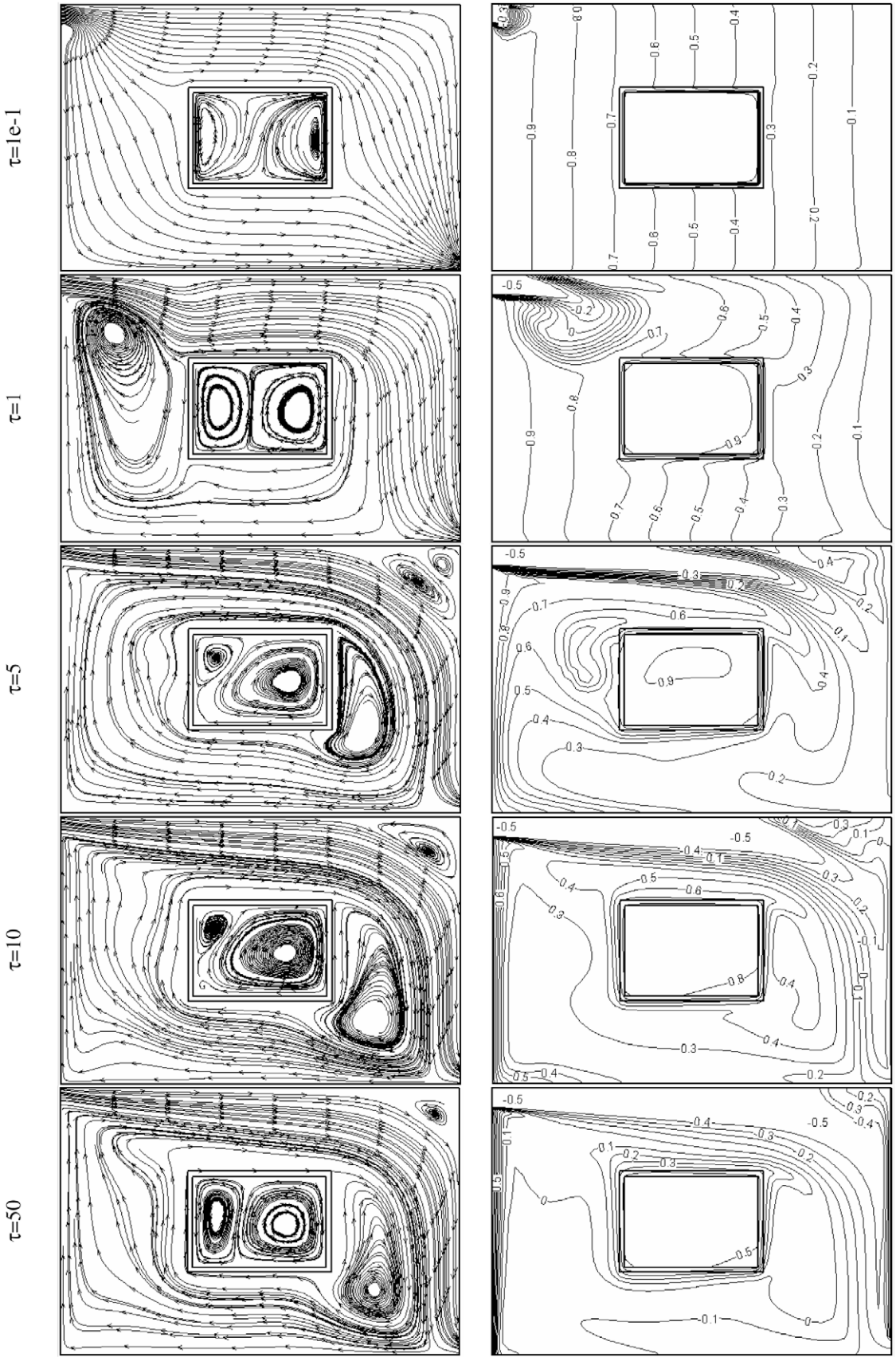

Fig. 7. Time variation of streamlines (left side) and distribution of temperature (right side), when the air in the container is cooled by water and Re = 500.

tigated by Deng and Tang, [19], for $10^3 \leqslant Ra \leqslant 10^6$ was the second limiting case studied. A qualitatively agreement was found for both streamlines and isotherms lines. As shown in Table 1, our predicted values of average Nusselt number agree to within 8%, with the results obtained by Deng and Tang, [19], with lower differences as the Reynolds number increases.

The mixed unsteady convection in a cavity with a centered thin walled solid container filled with an initially hot fluid is investigated by using the finite volume method, for Ri = 1 and Re = 200 and 500. Air and water are alternatively the fluids located inside and outside the inner container. Results obtained to describe fluid dynamics, in terms of streamlines along to the isotherms lines are presented in Figs. 4–7. Then, the two components velocity profiles results are shown in Fig. 8; dimensionless temperature spatial distributions in Fig. 9 and finally, local Nusselt numbers at the cavity vertical walls and on the inner container walls are presented.

Fig. 4 shows the evolution in time of the streamlines (on the left column) and isotherms (on the right column) for the case in which air enters into the cavity at a dimensionless temperature $\theta = -0.5$ and the centered inner container is filled with water at $\theta = 1$. Initially, at dimensionless time $\tau = 0.1$, air flows around the container without the presence of vortices, while inside the container with water two vortices can be noticed. For $\tau = 1$ a primary larger clockwise rotary vortex (CW) below the inlet flow and in the left section of the cavity and a second less developed vortex below the water container can be noticed in the external air flow. At time $\tau = 5$

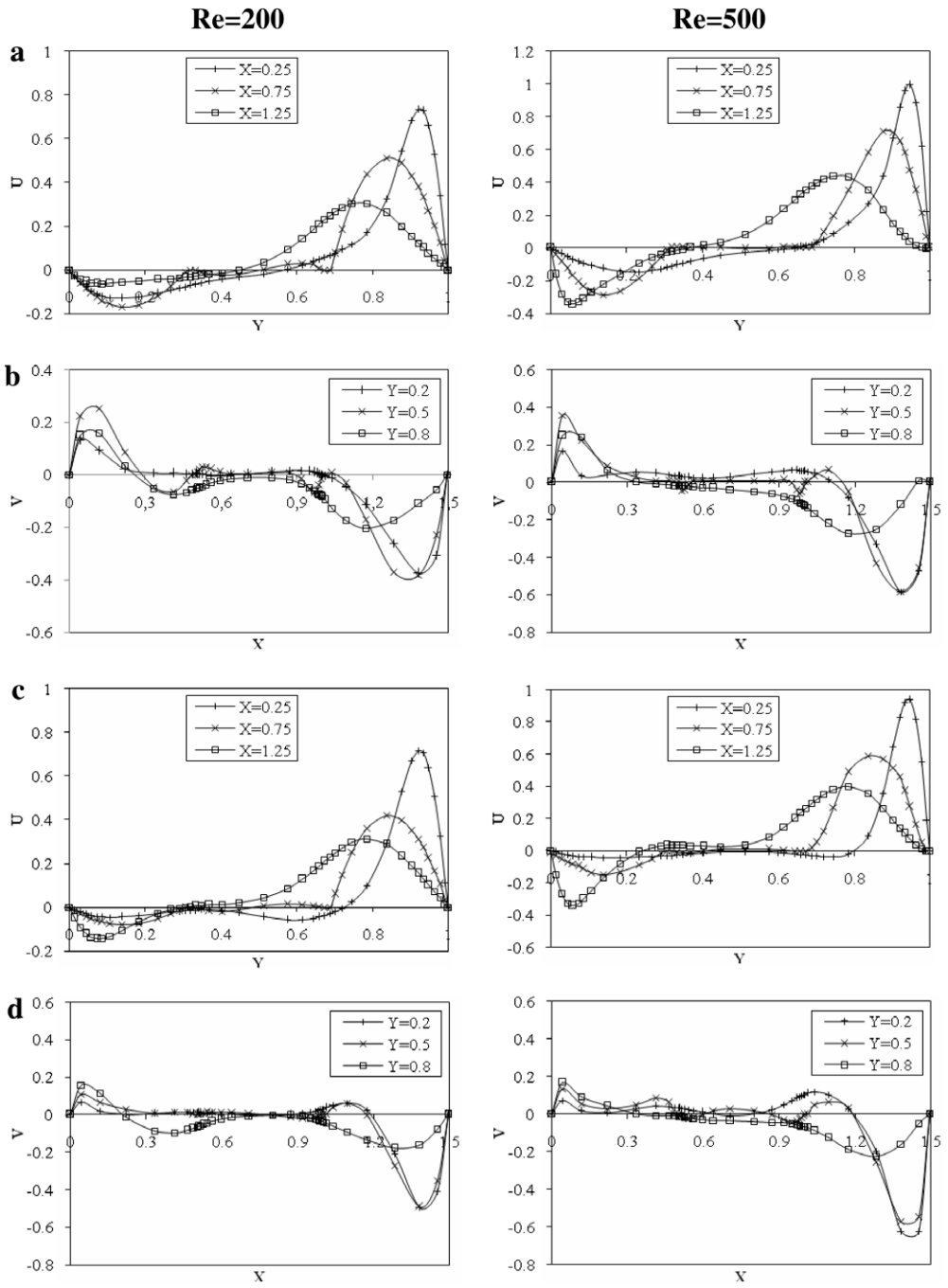

Fig. 8. Velocity profiles in vertical and horizontal cavity planes for water in the container cooled by air (a and b) and for air inside the container being cooled by water (c and d). Left column Re = 200, right column Re = 500.

the primary vortex in the surrounding air flow has moved down towards the inner container while the secondary vortex below the container is not longer present and a small vortex can be observed close to the right corner of the container. A pattern of air rotating clockwise around the inner container can be identified. The counter-clockwise rotating left vortex (CCW) and the clockwise rotating vortex in the inner water flow have moved towards the upper and lower container diagonal, respectively. At time $\tau = 10$, the left CCW rotating vortex in the inner water flow has decreased in size to one third of the container length while a small CCW rotating vortex has been developed in the upper part of the inner container. Finally, at the steady state $\tau = 50$, the inner water flows exhibits only one CCW rotating vortex while the external air flow shows the same flow circulation developed at $\tau = 5$. Time evolution of the isotherms slowly change from a diffusion controlled way at earlier times ($\tau = 0.1$) to a convective way for the air flow outside the inner container. Higher air temperature gradients are located near the inlet and towards the left hot wall of the cavity. Water in the internal container starts to cool down at $\tau = 1$. At time $\tau = 5$, only one third of the water have a temperature higher than 0.9 with larger temperature gradients close to the upper container wall.

The effect of inlet air velocity is studied next in Fig. 5, when the Reynolds number is 500. At earlier time, $\tau = 0.1$, external air and internal water flows are the same as those calculated for Re = 200, with very similar streamlines and isotherms lines. At $\tau = 1$, the lower CCW air circulating vortex captured for the

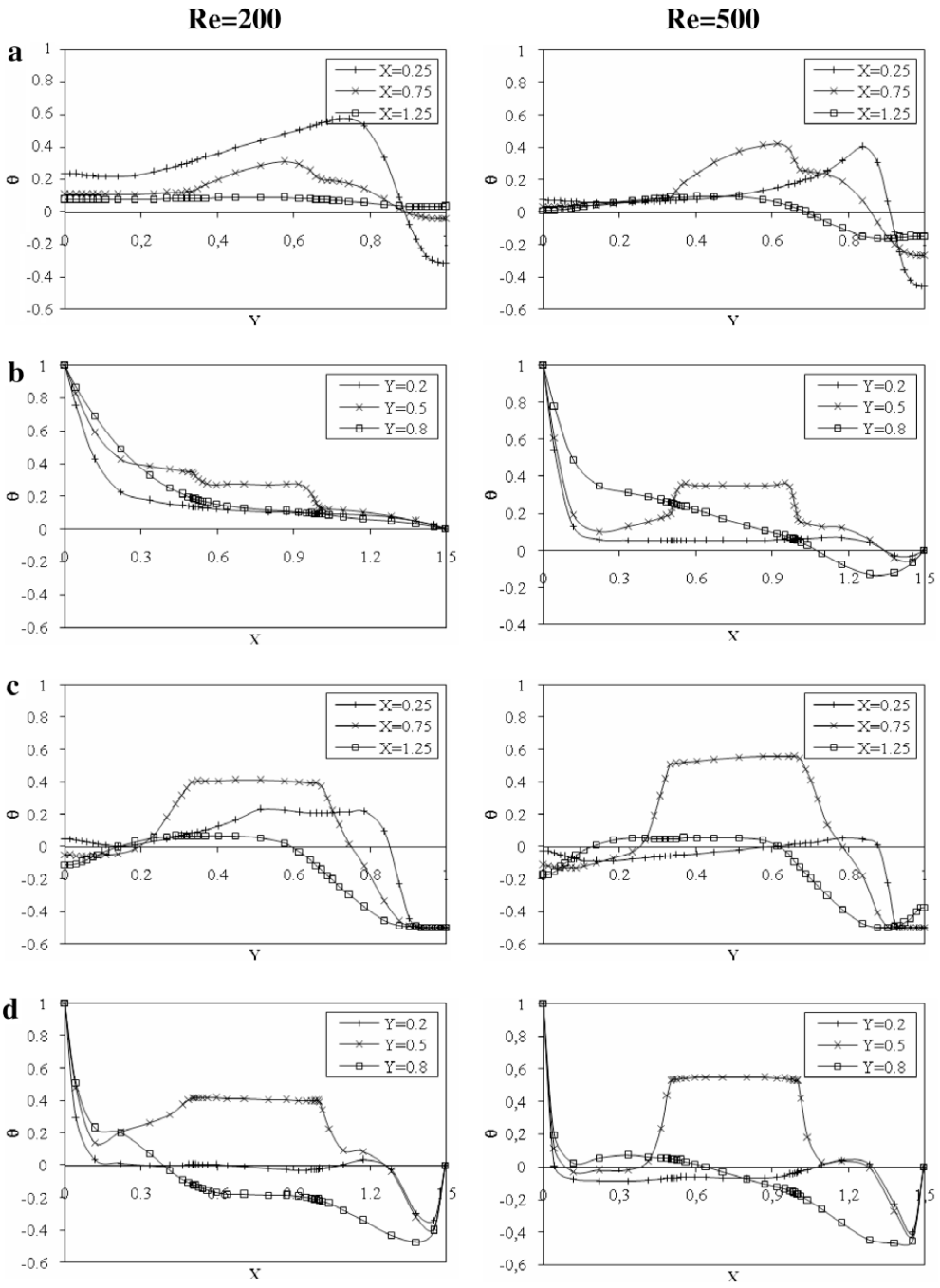

Fig. 9. Temperature profiles on vertical and horizontal planes for: (a and b) water in the container cooled by surrounding air and (c and d) air inside the inner container being cooled by water. Left column (Re = 200) and right column (Re = 500).

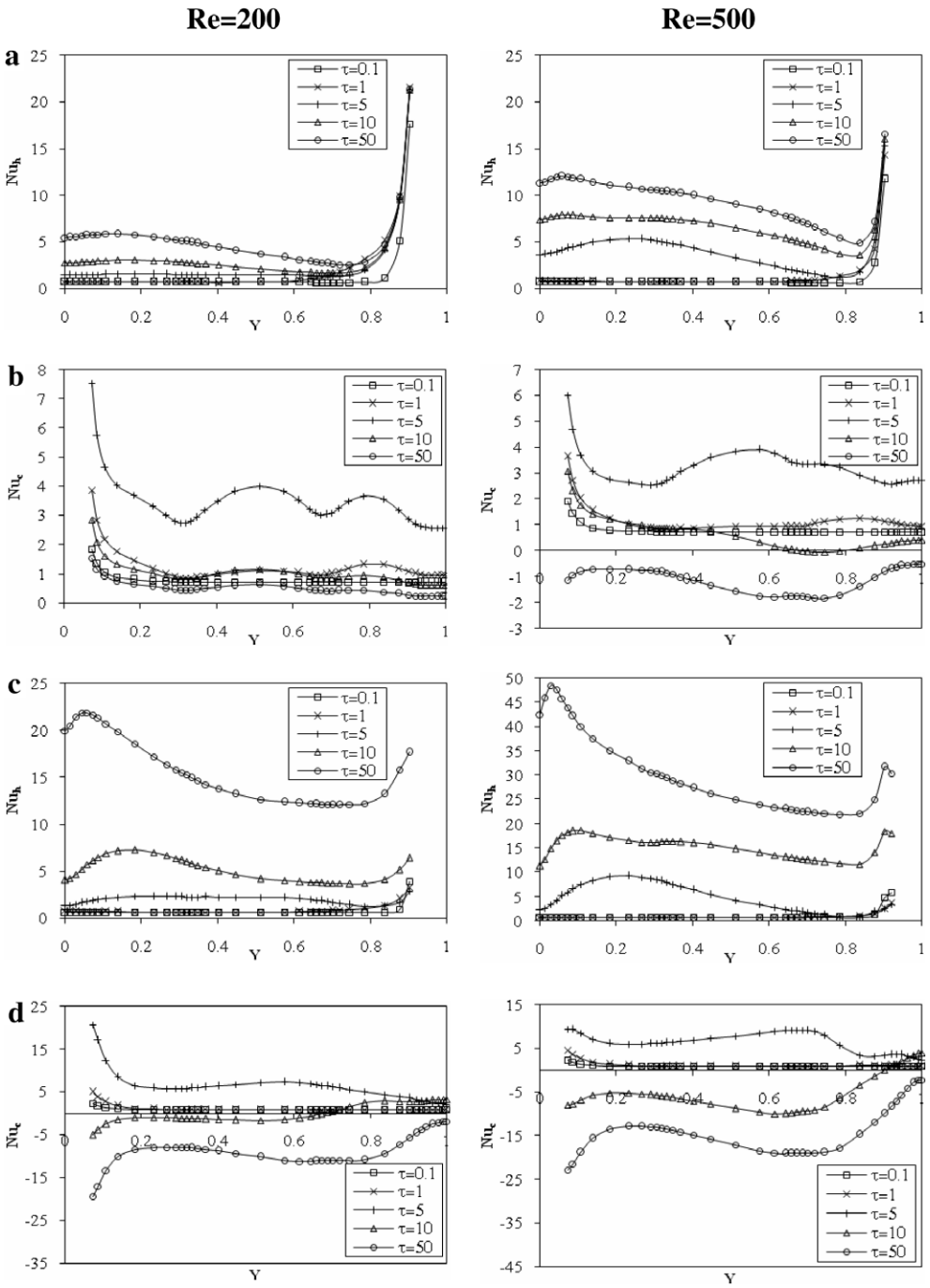

Fig. 10. Local Nusselt number on the vertical cavity walls for: (a and b) water cooled by air and (c and d) inner air cooled by water. Left column (Re = 200) and right column (Re = 500).

Re = 200 below the water container is not longer present. At a dimensionless time $\tau = 5$, the left CCW air rotating vortex at the left side of the cavity observed for the Re = 200 is not present and when Re = 500 it has been replaced for an air CCW rotating vortex located in the external lower right side of the water container, and two smaller vortices near the upper right cavity corner. Inside the inner container a similar trend in the water circulation is observed for the flows with Re = 200 and 500 up to $\tau = 5$. From then on the left water CCW rotating vortex is still important in size up to $\tau = 50$, when Re = 500.

The Reynolds number increment from Re = 200–500, keeping the Richardson number equal to 1, causes stratification in the air flow around the inner container that can be noticed starting from $\tau = 5$, in Fig. 5. The water cooling process slow down when Re = 500 and a higher water temperature inside the container can be observed for Re = 500 when $\tau > 5$.

Next, the case where air, located inside the centered inner container, is being cooled down by an external water flow is investigated. Fig. 6 depicts the streamlines and isotherms lines, at left and right sides, for Re = 200. Fluids mechanics of the external water flow and the internal convective flow of air are similar to previous results obtained when the water in the container was cooled by air, with Re = 200 (Fig. 4), when $\tau < 1$. Later, when $\tau = 5$, two secondary external vortices are formed in the upper right side of the cavity

caused by forced circulation of water. The primary vortex located near the inlet has been reduced in size in comparison with the streamlines shown in Fig. 4 for the external air/internal water case studied for Re = 200. The internal air circulation in the inner container shows at a dimensionless time $\tau = 5$ a main vortex which rotates in clockwise direction with one smaller counter-clockwise direction vortex located at the upper left side of the inner container. Later, for $\tau = 10$ and $\tau = 50$ only one secondary vortex can be seen in the upper right side of the cavity, that was not observed when the external fluid was water with an inner air fluid. Even though a similar trend is observed for the external water flow when $\tau \leqslant 1$, compared with the induced inner convective water flow caused by the external air flow when Re = 200 (Fig. 4) a faster cooling process for the inner contained fluid is obtained when water is cooled by air than when air is cooled by water.

Fig. 7 shows streamlines and isotherms when cold water enters the cavity with Re = 500 and air is filling the inner container. A similar trend in the external water circulation to the case when a cold air flow with Re = 500 circulates around the inner water container is observed. Inside the container air circulation shows at the end of the heating process ($\tau = 50$) a CCW vortex in the left side of the container and a larger CCW rotating vortex at the right side of the container that are similar to those vortices observed at time $\tau = 1$.

A slower cooling process for the inner air located inside the inner container occurs when water is circulated with Re = 500 than when water is being cooled down by an external air flow with Re = 500. The temperature stratification observed in the inner container with water for Re = 500 in Fig. 5, from time $\tau = 5$ on is no larger noticed when the inner container is filled with air for Re = 500.

Fig. 8a–d shows the horizontal (U) and vertical (V) velocity profiles for the four cases studied, at the steady state ($\tau = 50$) for Re = 200 (on the left) and Re = 500 (on the right). Velocity profiles are plotted along the vertical direction Y at three different location in the X-direction as $X = 0.25$, 0.75 and 1.25, while the vertical velocity profiles (V) are presented along the horizontal direction X, at three locations in the Y-direction as $Y = 0.2$, 0.5 and 0.8. As expected, the values of the external fluid velocity are increased as the Reynolds number increased with the maximum value of the velocity moving towards the cavity walls. A variation in the magnitude of the horizontal velocity in the region $0 \leqslant Y \leqslant 0.3$ at each one of the location $X = 0.25$, 0.75 and 1.25 in the X-direction was found when air circulated around the inner container filled with water, for Re = 200 (Fig 8a).

Variation of isotherms profiles with Reynolds number at three different location in X-direction ($X = 0.25$, 0.75 and 1.25) and at $Y = 0.2$, 0.5 and 0.8 in Y-direction are presented in Fig. 9a–d. When Fig. 9a–c are compared with each other, it is seen that the plane at $X = 0.25$ has a higher temperature for $0 \leqslant Y \leqslant 0.9$ and that the temperature is uniform at $X = 1.25$, when Re = 200 and air is flowing around the water (Fig. 9a). Temperature of the fluid, either air or water located inside the container is lower when Re = 200 than when Re = 500. The inspection of the temperature lines shows an improvement on heat transfer when air flows around the water container (Fig. 9a and b).

Fig. 10 shows the time evolution for the Nusselt number calculated in both hot and cold vertical walls, for Re = 200 and 500, when air flows around water (Fig. 10a and b) and when air in the container is being cooled down by an external water flow (Fig. 10c and d). As expected, higher Nusselt numbers in the hot wall are obtained for flows with Re = 500. Heat transfer from the hot wall to fluid increases when water is the external fluid, for either Re = 200 and 500. The local Nusselt number calculated on the cold wall increases with time until $\tau = 5$ and then decreases, reaching negative values that are higher when water flows around air and Re = 500.

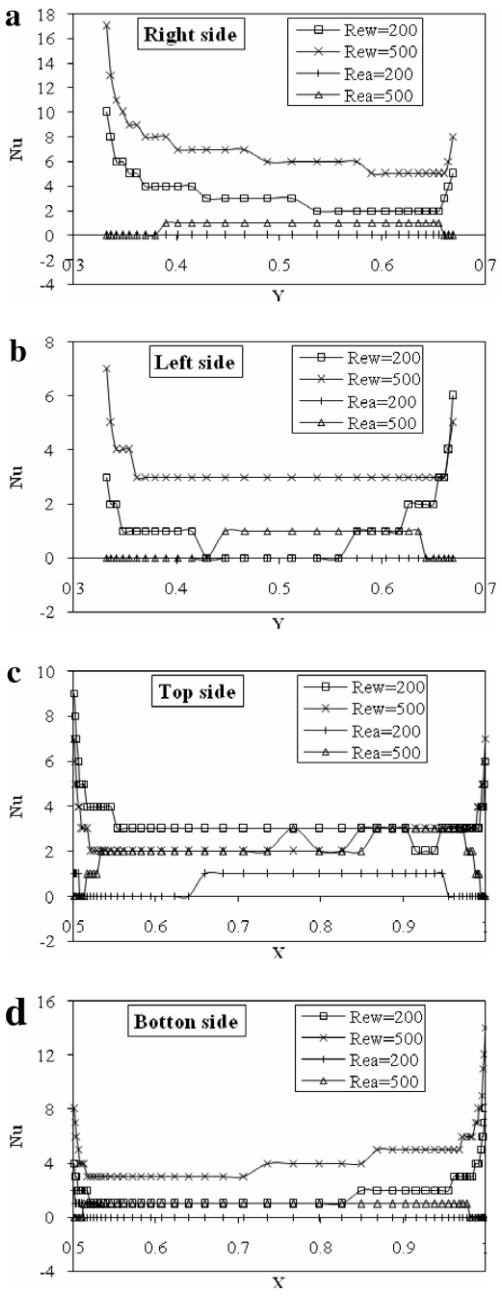

Fig. 11. Local Nusselt number on the inner container walls (Rew, inner air cooled by external water; Rea, inner water cooled by surrounding air).

Fig. 11a–d shows the local number in the final steady state for the four cavity walls of the inner container, for Re = 200, 500 and the two cases investigated: water cooled by air and air being cooled by water. Lower local Nusselt numbers are observed for air flowing around water, in comparison with the flow of water around air. Higher local Nusselt were calculated in the four walls for the flow with the higher Reynolds number, only with exception, on the top inner container wall when water was being used to cool down air (Fig. 11c, Re = 200).

6. Conclusion

Transient natural convection inside an inner rectangular container caused by external mixed convection, with Ri = 1, Re = 200 and 500, inside a square cavity has been investigated for either water

being cooled by air or air in the inner container being cooled by water. A higher heat transfer has been found when the external flow with Ri = 1 has a lower Reynolds number (Re = 200). As Re increases the external cold flow moves towards the walls of the external cavity away from the inner container walls. Natural convection in water located inside the inner container being cooled by mixed convection by a surrounding air laminar flow has a higher cooling rate than when air in the inner container is cooled by water. Enhanced heat transfer occurs at the right and bottom walls of the inner container, for the present situation, in which the coolant fluid enters to the cavity by the left upper side of the cavity and leaves the cavity by a port located in the lower side of the right wall.

Acknowledgement

The authors acknowledge CONICYT-Chile for support received in the FONDECYT 1070186 project.

References

[1] L.C. Fang, D. Nicolaou, J.W. Cleaver, Transient removal of a contaminated fluid from a cavity, Int. J. Heat Fluid Flow 20 (1999) 605–613.
[2] P. Verboven, A.K. Datta, N.T. Anh, N. Scheerlinck, B.M. Nicolai, Computation of airflow effects on heat and mass transfer in a microwave oven, J. Food Eng. 59 (2003) 181–190.
[3] R. Chu, Heat transfer in electronic system, in: Proceeding of Eighth International Heat Transfer Conference, San Francisco, CA, 1986, pp. 293–305.
[4] F.P. Incropera, Convection heat transfer in electronic equipment cooling, ASME J. Heat Transfer 110 (1988) 1097–1111.
[5] W. Nakayama, Thermal management of electronic equipment: a review of technology and research topics, in: A. Bar-Cohen, A.D. Kraus (Eds.), Advances in Thermal Modeling of Electronic Components and Systems, vol. 1, Hemisphere, 1988, pp. 1–78.
[6] S.S. Sathe, Y. Joshi, Natural convection liquid cooling of a substrate-mounted protrusion in a square enclosure: a parametric study, ASME J Heat Transfer 114 (1992) 401–409.
[7] M.M. Ganzarolli, L.F. Milanez, Natural convection in rectangular enclosure heated from below and symmetrically cooled from the sides, Int. J. Heat Mass Transfer 38 (6) (1995) 1063–1073.
[8] G.A. Lederma, A. Bejan, Optimal geometric arrangement of staggered vertical plates in natural convection, ASME J. Heat Transfer 119 (1997) 700–708.
[9] S. Armfield, R. Janseen, A direct boundary-layer stability analysis of steady-state cavity convection flow, Int. J. Heat Fluid Flow 17 (1996) 539–546.
[10] F.J. Hamady, J.R. Lloyd, Study of local natural convection heat transfer in an inclined enclosure, Int. J. Heat Mass Transfer 32 (9) (1989) 1697–1708.
[11] S.Z. Shuja, B.S. Yilbas, M.O. Budair, Natural convection in a square cavity with a heat generating body: entropy consideration, Heat Mass Transfer 36 (2000) 343–350.
[12] I. Dagtekin, H.F. Oztop, Natural convection heat transfer by heated partitions within enclosure, Int. Commun. Heat Mass Transfer 40 (2001) 823–834.
[13] S.H. Chuang, J.S. Chiang, Y.M. Kuo, Numerical simulation of heat transfer in a three-dimensional enclosure with three chips in various position arrangements, Heat Transfer Eng. 24 (2003) 42–59.
[14] M.T. Bhoite, G.S.V.L. Narasimham, M.V.K. Murthy, Mixed convection in a shallow enclosure with a series of heat generating components, Int. J. Therm. Sci. 44 (2005) 121–135.
[15] N. Yucel, A.H. Ozdem, Natural convection in partially divided square enclosure, Heat Mass Transfer 40 (2003) 167–175.
[16] X. Shi, J.M. Khodadadi, Laminar natural convection heat transfer in a differentially heated square cavity due to a thin fin on the hot wall, J. Heat Transfer 125 (2003) 624–634.
[17] S.H. Tasnim, M.R. Collins, Numerical analysis of heat transfer in a square cavity with a baffle on the hot wall, Int. Commun. Heat Mass Transfer 31 (2004) 639–650.
[18] Y. Varol, H. Oztop, T. Yilmaz, Natural convection in triangular enclosures with protruding isothermal heater, Int. J. Heat Mass Transfer 50 (2007) 2451–2462.
[19] Q. Deng, G. Tang, Numerical visualization of mass and heat transport for conjugate natural convection/heat conduction by streamline and heatline, Int. J. Heat Mass Transfer 45 (2002) 2373–2385.
[20] T.S. Chen, B.F.A. Maly, W. Aung, Mixed convection in laminar boundary layer flow, in: S. Kakac, W. Aung, R. Viskanta (Eds.), Natural Convection. Fundamentals and Applications, Hemisphere, Washington, DC, 1985.
[21] E. Papanicolau, Y. Jaluria, Mixed convection from an isolated heat source in a rectangular enclosure, Numer. Heat Transfer A 18 (1990) 427–461.
[22] E. Papanicolau, Y. Jaluria, Mixed convection from a localized heat source in a cavity with conducting walls: a numerical study, Numer. Heat Transfer A 23 (1993) 463–494.
[23] E. Papanicolau, Y. Jaluria, Computation of turbulent flow in mixed convection in a cavity with a localized heat source, ASME J. Heat Transfer 117 (1995) 649–658.
[24] S.C. Lee, C.Y. Cheng, C.K. Chen, Finite element solutions in laminar and turbulent flows with forced and mixed convection in an air-cooled room, Numer. Heat Transfer A 31 (1997) 529–550.
[25] A. Raji, M. Hasnaoui, Mixed convection heat transfer in a rectangular cavity ventilated and heated from the side, Numer. Heat Transfer A 33 (1998) 533–548.
[26] A. Raji, M. Hasnaoui, Correlations en convection mixte dans une pièce ventilée, Rev. Gén. Therm. 37 (1998) 874–884.
[27] A. Raji, M. Hasnaoui, Mixed convection heat transfer in ventilated cavities with opposing and assisting flows, engineering computation, Int. J. Comput.-Aided Eng. Softw. 17 (5) (2000) 556–572.
[28] A. Raji, M. Hasnaoui, Combined mixed convection and radiation in ventilated cavities, engineering computations, Int. J. Comput.-Aided Eng. Softw. 18 (7) (2001) 922–949.
[29] A. Omri, S.B. Nasrallah, Control volume finite element numerical simulation of mixed convection in an air-cooled cavity, Numer. Heat Transfer A 36 (1999) 615–637.
[30] N. Moraga, S. López, Numerical simulation of three-dimensional mixed convection in an air-cooled cavity, Numer. Heat Transfer A (2004) 811–824.
[31] S.M. Saeidi, J.M. Khodadadi, Forced convection in a square cavity with inlet and outlet ports, Int. J. Heat Mass Transfer 49 (2005) 1896–1906.
[32] S.Z. Shuja, B.S. Yilbas, M.O. Iqbal, Mixed convection in a square cavity due to heat generating rectangular body. Effect of cavity exit port locations, Int. J. Numer. Methods Heat Fluid Flow 10 (2000) 824–841.
[33] S.V. Patankar, Numerical Heat Transfer and Fluid Flow, Hemisphere, Washington, DC, 1980.